

Batool et al., 2024 (08-06-2024)

by Fatima Batool

Submission date: 07-Jun-2024 07:28PM (UTC-0700)

Submission ID: 2397986886

File name: Manuscript_Excluding_References_and_Declarations.docx (176.71K)

Word count: 5054

Character count: 28450

ORIGINALITY REPORT

14%

SIMILARITY INDEX

7%

INTERNET SOURCES

9%

PUBLICATIONS

1%

STUDENT PAPERS

PRIMARY SOURCES

- 1 Muhammad Noman, Muhammad Shahid, Temoor Ahmed, Muhammad Bilal Khan Niazi, Sabir Hussain, Fengming Song, Irfan Manzoor. "Use of biogenic copper nanoparticles synthesized from a native Escherichia sp. as photocatalysts for azo dye degradation and treatment of textile effluents", Environmental Pollution, 2020
Publication 2%
- 2 www.mdpi.com
Internet Source 2%
- 3 Environmental Science and Engineering, 2015.
Publication 1%
- 4 Irfan Haidri, Muhammad Shahid, Sabir Hussain, Tanvir Shahzad et al. "Efficacy of Biogenic Zinc Oxide Nanoparticles in Treating Wastewater for Sustainable Wheat Cultivation", Plants, 2023
Publication 1%
- 5 Faisal Mahmood, Muhammad Shahid, Sabir Hussain, Tanvir Shahzad et al. "Potential plant 1%

growth-promoting strain *Bacillus* sp. SR-2-1/1
decolorized azo dyes through NADH-
ubiquinone:oxidoreductase activity",
Bioresource Technology, 2017

Publication

6

www.researchsquare.com

Internet Source

1 %

7

Khadija Siddique, Muhammad Shahid, Tanvir
Shahzad, Faisal Mahmood et al. "Comparative
efficacy of biogenic zinc oxide nanoparticles
synthesized by *Pseudochrobactrum* sp. C5
and chemically synthesized zinc oxide
nanoparticles for catalytic degradation of
dyes and wastewater treatment",
Environmental Science and Pollution
Research, 2021

Publication

1 %

8

Submitted to Higher Education Commission
Pakistan

Student Paper

1 %

9

ia801205.us.archive.org

Internet Source

1 %

10

fatcat.wiki

Internet Source

<1 %

11

pubs.rsc.org

Internet Source

<1 %

c.coek.info

12

Internet Source

<1 %

13

Xiaoxuan Wang, Jinming Jiang, Weijun Gao. "Reviewing textile wastewater produced by industries: characteristics, environmental impacts, and treatment strategies", *Water Science and Technology*, 2022

Publication

<1 %

14

publications.waset.org

Internet Source

<1 %

15

www.frontiersin.org

Internet Source

<1 %

16

www.ias.ac.in

Internet Source

<1 %

17

Fereshteh Jabalameli, Mohammad Emaneini, Reza Beigverdi, Shahnaz Halimi, Maryam Siroosi. "Determining effects of nitrate, arginine, and ferrous on antibiotic recalcitrance of clinical strains of *Pseudomonas aeruginosa* in biofilm-inspired alginate encapsulates", *Annals of Clinical Microbiology and Antimicrobials*, 2023

Publication

<1 %

18

mail.journalcra.com

Internet Source

<1 %

19

rmebrk.kz

Internet Source

<1 %

20

thesis.asianindexing.com

Internet Source

<1 %

21

www.ncbi.nlm.nih.gov

Internet Source

<1 %

22

Gerry Aplang Jana, Mahmoud W. Yaish.
"Isolation and functional characterization of a
mVOC producing plant-growth-promoting
bacterium isolated from the date palm
rhizosphere", Rhizosphere, 2020

Publication

<1 %

23

ftp.academicjournals.org

Internet Source

<1 %

24

innovareacademics.in

Internet Source

<1 %

25

repository.ju.edu.et

Internet Source

<1 %

26

researchonline.ljmu.ac.uk

Internet Source

<1 %

27

www.researchgate.net

Internet Source

<1 %

28

www.science.gov

Internet Source

<1 %

www.studymode.com

30

A. Sezai Sarac, Murat Ates, Elif Altürk Parlak. "Comparative Study of Chemical and Electrochemical Copolymerization of N-Methylpyrrole with N-Ethylcarbazole Spectroscopic and Cyclic Voltammetric Analysis", International Journal of Polymeric Materials, 2005

Publication

<1 %

31

Jang, Gyoung Gug, Christopher B. Jacobs, Ryan G. Gresback, Ilia N. Ivanov, Harry M. Meyer, III, Michelle Kidder, Pooran C. Joshi, Gerald E. Jellison, Tommy J. Phelps, David E. Graham, and Ji-Won Moon. "Size tunable elemental copper nanoparticles: extracellular synthesis by thermoanaerobic bacteria and capping molecules", Journal of Materials Chemistry C, 2014.

Publication

<1 %

32

Vahideh Mohammadzadeh, Mahmood Barani, Mohammad Sadegh Amiri, Mohammad Ehsan Taghavizadeh Yazdi et al. "Applications of plant-based nanoparticles in nanomedicine: A review", Sustainable Chemistry and Pharmacy, 2022

Publication

<1 %

Exclude quotes Off

Exclude matches Off

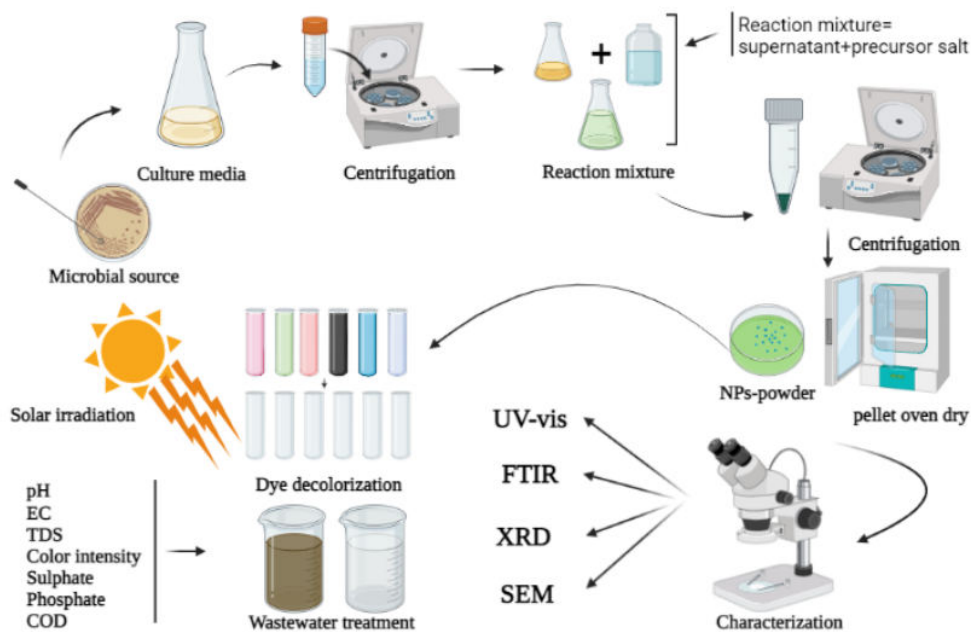
Exclude bibliography Off

9 ¹
1 Biosynthesis of copper nanoparticles using *Bacillus flexus* and estimation of their potential for
2 decolorization ¹ of azo dyes and textile wastewater ¹ treatment

3 **Abstract**

4 In many underdeveloped countries, textile industries discharge their effluents without any
5 treatment. The untreated textile wastewater consists of both azo dyes and heavy metals which
6 not only change the physicochemical and biological properties of soil and water but also affect
7 human health. In recent years, copper-based nanomaterials have attained worldwide attention
8 because of their unique properties and potential for decolorization of azo dyes and wastewater
9 treatment. ¹⁸ The present study demonstrates the bacterial synthesis of copper nanoparticles (Cu-
10 NPs) using *Bacillus flexus* strain isolated from a textile wastewater followed by their
11 application for ¹ photocatalytic degradation of various azo dyes and treatment of actual
12 wastewater. ⁶ The FT-IR analysis confirmed the presence of various functional groups including
13 proteins on Cu-NPs which improved their stability. ¹¹ The scanning electron microscopy (SEM)
14 images revealed the spherical shape of Cu-NPs with a size of range between 17-34 nm.
15 Similarly, the XRD analysis of biosynthesized Cu-NPs showed various diffraction peaks at
16 44.5°, 51.5°, 74.75 which confirmed ¹ the crystalline nature of nanoparticles. While studying the
17 ¹ photocatalytic decolorization of azo dyes by Cu-NPs, it was observed that 88.164 ± 0.19 %,
18 88.452 ± 1.89 %, 90.433 ± 1.81 %, 64.770 ± 1.02 %, 46.774 ± 1.61 %, and 67.274 ± 2.89 % of
19 reactive black-5, congo red, malachite green, methylene blue, reactive red-2 and blue direct,
20 respectively, were decolorized after 4 hours of solar irradiation at 50 ppm concentration.
21 Additionally, the biosynthesized nanoparticles also resulted in reduction of various parameters
22 like EC, pH, TDS, COD, color intensity, sulphates, and phosphates in the textiles wastewater.
23 The reduction of COD, sulfates, and phosphates was about 39.659 %, 43.157 %, and 49.493
24 ⁷ %. The results of current work suggest that biosynthesized copper nanoparticles might serve as

25 a potential green solution for the decolorization of various dyes including wastewater
26 treatment.



28 **Key words:** Bacterial isolation, Biosynthesis, Copper nanoparticles, Photocatalysis, Dye
29 degradation, Wastewater treatment

30 **Abbreviations:** Biological oxygen demand (BOD), Chemical oxygen demand (COD),
31 Electrical conductivity (EC), Copper nanoparticles (Cu-NPs), Ultraviolet visible spectroscopy
32 (UV-vis), Scanning electron microscopy (SEM), Fourier transform infrared spectroscopy
33 (FTIR), X-ray diffraction (XRD)

34 1. Introduction

35 Water is one of the most important natural resource on earth not only for human beings but
36 also for all other living organisms. All essential phenomena of the biosphere depend on the
37 availability of water. Along with other human requirements, a huge amount of water is also
38 used for industrial processes. Among different industries, the textile industries utilize an

39 enormous amount of water for different activities such as dyeing and washing and similarly
40 this untreated water becomes part of the environment as wastewater (Imran et al., 2015). It is
41 reported that, after dyeing one kilogram (Kg) of fabric, about 40-65 L of wastewater is
42 produced (Balarak et al., 2019). Approximately 20 % of applied quantity of different dyes is
43 lost during the process of washing and dyeing and discharged along with wastewater (Fathima
44 et al., 2018). The major problem with untreated textile wastewater is its color due to ²⁵the
45 presence of these dyes in large quantities. It is reported that dyes have many carcinogenic and
46 mutagenic properties. Moreover, several environmental problems such as elevation of various
47 parameters like pH, BOD, suspended bodies, and COD of aquatic bodies are associated with
48 untreated textile effluents ⁵(Imran et al., 2015, Subramaniam et al., 2022; Bilal et al., 2023).
49 Thus, dyes loaded textile wastewaters limits downstream usage such as drinking, washing,
50 irrigation, and recreation (Imran et al., 2015).

51 Many physical (adsorption, membrane filtration, coagulation and filtration method),
52 chemical (oxidation like chlorination, ozonation, bleaching and advanced oxidation method
53 with heterogenous and homogenous catalysts) and biological (employing bacteria, fungi, yeast,
54 algae, and plants) methods ³have been used for the treatment of dyes loaded textile wastewater
55 (Singh et al., 2017). Above mentioned physiochemical methods are associated with many
56 drawbacks such as they are expensive and make use of dangerous chemicals. Furthermore, they
57 are also a source of secondary pollutants such as production of sludge (Bharagava et al., 2020).
58 In contrast, biological methods are environmentally-friendly and even they have ability to
59 completely mineralize many azo dyes. Many reports have described ³the role of microorganisms
60 ⁵in the removal of azo dyes from textile effluents (Hussain et al., 2013, Thangaraj et al., 2021).
61 Microorganisms ³involved in decolorization of azo dyes produce many ¹³enzymes such as azo
62 ⁵reductase, laccase, peroxidase, MG reductase, and aminopyrine N-demethylase (Souza et al.,
63 2022). ⁵However, the rate of biodegradation process depends on many factors including survival

64 activity, and adaptability of microbes with chemical properties of azo dyes and other
65 xenobiotics (Manjarrez et al., 2021). Although biological methods are eco-friendly but the old
66 methods may not be much effective to fulfill the strict standards of water quality and to remove
67 emergent contaminants.

68 During the past few years, use of nanomaterials has attained worldwide attention for
69 the degradation of various dyes. They are preferred because of production of biodegradable
70 end products such as aromatic amines which can be further biodegraded easily by microbes
71 (Nazar et al., 2018). Various studies have highlighted the catalytic potential of different metal
72 nanoparticles including silver, titanium, zinc and nickel nanoparticles for the decolorization of
73 different dyes (Edison et al., 2016, Saravanan et al., 2017, Kiran et al., 2020, Mustafa et al.,
74 2023). Among other metal nanoparticles, copper nanoparticles are of excessive interest because
75 of their low cost, availability, and unique properties such as catalytic, antibacterial, biocidal,
76 optical, magnetic and heat transfer abilities (Punniyakotti et al., 2020, Ghaffar et al., 2021).
77 Furthermore, in comparison to silver-nanoparticles, copper nanoparticles (Cu-NPs) have more
78 chemical and physical stability and ease of mixing with polymers (Palani et al., 2022). The Cu-
79 NPs find their applications in many fields like health (antibacterial, anticancer, dentistry, etc.),
80 food and agriculture (antifungal, nano herbicides, nano-fertilizers, improving texture, etc.),
81 industry (nano composites, cosmetics, nano-pigments, paper coating) and environment (nano
82 remediation, wastewater treatment, biodegradation of polymer, environmental catalysts, etc.)
83 (Ball et al., 2019). For example, Cu-NPs have the ability for dechlorination of dichloromethane
84 (a ground water contaminant) with NaBH₄ by using them as catalyst (Huang et al., 2012). They
85 showed 90% reduction of dichloromethane within 1 hour using NaBH₄ and no degradation was
86 observed without NaBH₄ (Huang et al., 2012).

87 Different physical and chemical methods like precipitation-pyrolysis method,
88 sonochemistry, cathodic vacuum arc and solvothermal reactions have been reported for

89 physicochemical synthesis of copper-based nanoparticles (Botsa et al., 2019). All such methods
90 make use of the chemicals which make them eco-hazardous and avoid their applications in
91 other fields of clinical, medicine and biology (Akintelu et al., 2020). So, the researchers are
92 more interested toward biological method for nanoparticles synthesis because of the above-
93 mentioned problems that are associated with physicochemical methods. Numerous bacterial
94 species are reported to synthesize copper nanoparticles like *Salmonella typhimurium* (Ghorbani
95 et al., 2015), *Shewanella oneidensis* (Kimber et al., 2018), *Halomonas elongate* (Rad et al.,
96 2018), *Streptomyces* sp. (Hassan et al., 2019), *Escherichia coli* (Zaynitdinova et al., 2020),
97 *Pseudomonas stutzeri* (Zaynitdinova et al., 2020), *Pseudomonas fluorescens* (Bayat et al.,
98 2021). Similarly, various studies have highlighted the capability of copper nanoparticles in
99 facilitating the photocatalytic degradation of different dyes (Fathima et al., 2018, Noman et al.,
100 2020). For wastewater treatment, Anjum et al. (2019) described the nanotechnology as one of
101 the most advanced process. In this backdrop, following research investigates an innovative and
102 sustainable approach for synthesizing Cu-NPs. The potential of bacterial strain was harnessed
103 with an aim to not only reduce the environmental impact but also enhance its cost effectiveness.
104 For in-depth understanding of Cu-NPs, various cutting-edge techniques such as, UV-Vis
105 spectroscopy, FTIR, SEM, and XRD were used. This study was not only focused on green
106 synthesis but also holds an immense promise in catalytic biodegradation of various azo-dyes.
107 Furthermore, the potential of nanoparticles for the treatment of textile waste water was also
108 explored, thus contributing to environmental conservation. This is the research that promises
109 to not only captivate but also contribute to a greener and more sustainable future.

110

111 **2. Materials and Methods**

112 **2.1 Materials**

113 All the reagents or chemicals namely nutrient agar, nutrient broth, and copper sulfate
114 pentahydrate, used for experimental analysis, were procured from Sigma Aldrich or UNI-Chem
115 and used without any purification techniques. The dyes used in this study namely congo red
116 (CR), reactive black-5 (RB-5), methylene blue (MB), reactive red-2 (RR-2), and blue direct
117 (BD) were also purchased from Sigma Aldrich. Moreover, the glassware used during
118 experimental analysis was washed with distilled water and autoclaved.

119 2.2 Collection of Samples for the Isolation of Bacterial Strain

120 Wastewater samples were collected from Five-star Textile Industry Faisalabad. Bacterial
121 strains were isolated using serial dilution method. Dilutions (10^{-4} to 10^{-6}) were spread on plates
122 of nutrient agar amended with the solution of copper sulfate (1 mM). These plates were
123 incubated for 48 hours in incubator at 30 °C. The bacterial colonies having ability to tolerate
124 stress were purified by repeated streaking method on freshly prepared plate and labelled.
125 Among different isolates, strain FB-1 was used for the biosynthesis of nanoparticles.

126 2.3 Biosynthesis of Copper Nanoparticles

127 For the biosynthesis of copper nanoparticles (Cu-NPs), the colony of bacterial strain was
128 inoculated in nutrient broth medium along with two controls (The first control containing only
129 the uninoculated medium and the second control containing the uninoculated medium along
130 with the precursor salt), and incubated under shaking condition at 120 rpm for 48 hours at 28
131 °C. The culture was centrifuged for 10 minutes at 7000 rpm to remove the pellet for
132 extracellular synthesis of Cu-NPs. The supernatant was then added with 10 mM copper sulfate
133 pentahydrate solution and incubated again under shaking condition for 24 hours at 120 rpm.
134 Equal concentration of precursor salt solution was also added to the second control. The change
135 in color from bluish-to-bluish green in comparison to control confirmed the biosynthesis of
136 Cu-NPs. The reaction mixture was again subjected to centrifugation for about 10 minutes at
137 7000 rpm at 4°C to remove the supernatant. The pellet was washed with double distilled water

138 to remove the impurities and placed in an oven to heat dry the nanoparticles. They were then
139 ground into fine powder.

140 **2.4 Molecular Characterization and Phylogenetic Study**

141 The selected bacterial isolate having potential of Cu-NPs synthesis was identified on molecular
142 basis. The 16 S rRNA gene was amplified using forward and reverse primers f-D1 (5'-
143 AGAGTTTGATCCTGGCTCAG-3') and r-D1 (5'-AAGGAGGTGATCCAGCC-3')
144 (Weisburg et al., 1991). The amplified gene products of 16 S rRNA were sequenced
145 commercially by Macrogen, South Korea. The retrieved sequence of 16 S rRNA gene was
146 trimmed analyzed by Sequence Scanner software package and trimmed on both sides to cut the
147 bad sequences. The BLASTn was used for identification of strain. Then the phylogenetic tree
148 was constructed by using NJ (neighbour-joining) method to describe the identity of selected
149 strain.

150 **2.5 Characterization of Biosynthesized Copper Nanoparticles**

151 The bacterial synthesis of Cu-NPs was confirmed using Ultraviolet Visible Spectroscopy
152 (Shimadzu, Kyoto, Japan). It determined the maximum absorption spectra of samples. UV-vis
153 spectroscopy analyzed the reaction mixture at a wavelength ranging from 300-800 nm (Noman
154 et al., 2020).

155 Scanning Electron Microscopy (SEM) was employed to describe the shape and surface texture
156 of biosynthesized Cu-NPs (Instrument: JSM-6490). SEM was conducted by following the
157 method of Tiwari et al., (2016). For SEM analysis, about 10 µL of homogenous cell free
158 colloidal solution was placed on cover slip made up of glass and dried at 100 °C. After that,
159 the glass cover slip was cooled and fixed on aluminum stub using adhesive carbon tape.

160 The crystalline nature of biosynthesized nanoparticles was determined using X-ray
161 diffraction analysis. To determine the XRD pattern, the drop was coated on glass substrate and
162 placed in X-ray diffractometer apparatus (JCPDS Card #=04-0836) which was operated at 40

163 mA and 45 KV voltage of current with Cu K α rays. The crystalline nature of biosynthesized
164 nanoparticles was analyzed, and Debye-Scherrer's formula, was used for their average size
165
$$(D=K\lambda/\beta \cos\theta)$$

166 Whereas,

167 D = "Crystalline size", K = "Sharrer's constant" and its value is "0.9", λ = Wavelength of "x-
168 ray source", β = "Width at 1/2 maximum of reflection peaks" and, θ = "Peak position".

169 Functional groups and associated proteins that participate in stability of biosynthesized Cu-
170 NPs were determined by Fourier-Transform Infrared Spectroscopy (FT-IR) (FTIR-Bruker
171 TENSOR- 27). The dried powder of biosynthesized Cu-NPs was taken to FTIR measurement
172 and the FTIR spectra were attained. It is useful method to ascertain the various type of chemical
173 bonds in a molecule by making an IR absorption spectrum that functioned as molecular
174 fingerprint. The analysis of FT-IR was conducted in a range of 4000 to 350 cm^{-1} .

175 **2.6 Catalytic Degradation of Azo Dyes**

176 **2.6.1 Optimization of Concentration of Cu-NPs for RB-5 Decolorization**

177 Various concentrations of Cu-NPs were used to check their potential of decolorization of RB-
178 5. 50 ppm concentration of RB-5 was used for this purpose. Various concentrations of NPs
179 such as (0.05, 0.1, 0.2, 0.5, 1, 2, 3, 4, 5 and 10 mg ml^{-1}) were added to the solution of RB-5 and
180 placed in solar irradiation for 4 hours after shaking for about 10 minutes. After each hour, 1 ml
181 of sample was taken from each concentration in a 1.5 ml Eppendorf tube. The samples were
182 centrifuged for about 10 minutes at 7000 rpm to remove the Cu-NPs. Spectrophotometer was
183 used to check the ability of different concentrations of nanoparticles by measuring the
184 decolorization of RB-5. The optimized concentration (0.5 mg ml^{-1}) of Cu-NPs was used for
185 further analysis.

186 **2.6.2 Decolorization of Azo Dyes Using Optimized Concentration of NPs**

187 The optimized concentration (0.5 mg ml⁻¹) of nanoparticles was used for the decolorization of
188 various other dyes such as MB, RB-5, BD, CR, MG, and RR-2 dyes at 25 and 50 ppm
189 concentrations. For this purpose, optimized concentration of biosynthesized Cu-NPs (50 mg)
190 was added to the solution (100 ml) of above-mentioned azo dyes. The reaction mixtures were
191 then placed in sun light for incubation for about 4 hours. 1 ml of sample was taken from each
192 dye in 1.5 mL Eppendorf tube after specific time interval. The Eppendorf tubes containing
193 samples were centrifuged for 10 minutes at 7000 rpm to remove the Cu-NPs.
194 Spectrophotometer was used to evaluate the degradation of dyes. The decolorization of dyes
195 namely MB, CR, BD, RR-2, RB-5, and MG was evaluated at 561, 478, 592, 540, 597, and 624
196 nm, respectively. The %age of dyes degradation was calculated using the formula written
197 below,

$$198 \quad \% \text{ decolorization} = ((C-S) \times C) / 100$$

199 Whereas,

- 200 • C is control
- 201 • S is sample

202 2.6.3 Treatment of Wastewater

203 Bacterial synthesized Cu-NPs were also used for the treatment of actual wastewater. The
204 sample of wastewater was collected from paharang drain (North-31.526904 and East-
205 73.118483) and Sargodha Road, Faisalabad, Pakistan. It was firstly centrifuged at 10,000 rpm
206 for 5 minutes to remove the particulate matter. The collected wastewater was spiked with congo
207 red (50 ppm) to have considerable concentration of the dye and color intensity. 50 mg (0.5 mg
208 ml⁻¹) of biosynthesized Cu-NPs were then added to 100 ml of wastewater by keeping the
209 control without nanoparticles to evaluate the treatment of wastewater. Sample was vortexed
210 and incubated in the presence of sunlight for about 7 hours. After incubation, the samples were
211 centrifuged for 10 minutes at 7000 rpm to remove the Cu-NPs. Different parameters like pH,

212 chemical oxygen demand, electrical conductivity, phosphates, color intensity, and sulphates
213 were checked before and after the treatment following the procedure described by Rump,
214 (1999) and Maqbool ²⁶ et al., (2016).

215 **2.7 Statistical Analysis**

216 The experimental data of treatment was entered in Microsoft Excel 2016, and percentage
217 decolorization, means, and standard deviation was calculated. For analyzing data, completely ⁴
218 randomized design was used. Analysis of variance was calculated by using statistix 8.1 ²
219 software. Principle component analysis and heat map was also constructed using the R-studio ²
220 (Version 4.2.2).

221 **3. Results and Discussion**

222 **3.1 Isolation, Molecular Characterization and Phylogenetic Analysis**

223 The selected isolate was purified by repeated streaking method on freshly prepared nutrient
224 agar plates until single colony was obtained. The growth pattern of selected isolate on nutrient
225 agar plate media has been represented in the Figure S1. The phylogenetic analysis of 16 S
226 rRNA gene and BLASTn of isolate determined that the selected isolate belongs to genus
227 *Bacillus*. In Phylogenetic tree (Figure 1), selected strain clustered with *Bacillus* spp. ¹ The 16S
228 rRNA gene sequence of strain (FB-1) was also compared with known sequences in database
229 ¹ using BLASTn program of NCBI and the sequence showed more than 99 % resemblance with
230 the bacterial strains belonging to genus *Bacillus*.

231

232 **3.2 Biosynthesis and Characterization of Copper Nanoparticles**

233 Various microbial isolates have been reported describing the synthesis of Cu-NPs. In this study
234 *Bacillus* spp. Strain FB-1 was used for the extracellular synthesis of Cu-NPs at 10 mM
235 concentration of copper sulphate salt. On addition of salt, the change in color (from bluish to
236 blue greenish) firstly confirmed the biosynthesis process (Figure 2A). Similar result was

237 reported earlier by Tiwari et al. (2016) who synthesized Cu-NPs using *Bacillus cereus* strain
238 at 10 mM concentration of copper sulfate salt. On the other hand, Noman et al., (2020) also
239 reported the bacterial synthesis of Cu-NPs using *Escherichia* sp. strain SINT7 at 5 mM
240 concentration of precursor salt. The *Bacillus flexus* strain was also used for the synthesis of
241 silver nanoparticles (Priyadarshini et al., 2013). Furthermore, several other nanoparticles such
242 as cadmium sulphide (Singh et al. 2011), iron oxide (Sundaram et al. 2012), titanium dioxide
243 (Khan and Fulekar, 2016) and zinc oxide (Hamk et al. 2023) were synthesized from *Bacillus*
244 spp. Hence, the bacterial strain *Bacillus* spp. FB-1 is a new addition as a bacterial member for
245 the synthesis of nanoparticle.

246 The change in color was the first confirmation of biosynthesis of Cu-NPs. The cell free
247 reaction mixture showed absorbance peak at 325 nm using UV-vis spectrophotometer which
248 confirmed the synthesis of Cu-NPs as depicted in Figure 2B. Similar result was reported by
249 Noman et al. (2020) and concluded that peak in this region confirmed the reduction of precursor
250 salt into nanoparticles. Moreover Singh et al. (2010) and Mamuru et al. (2018) also reported
251 the confirmation peak of Cu-NPs at 310 nm. While Fathima et al., (2018) and Hassan et al.
252 (2019) showed an absorption peak at 560 and 590 nm.

253 The SEM analysis revealed the morphology of biosynthesized Cu-NPs. The SEM
254 image of the biosynthesized Cu-NPs (Figure 3) indicated that the sample contained copper
255 nanoclusters with irregular spherical shape and present in an agglomerated form. The analysis
256 of SEM images revealed that the particles size was in range of 17-34 nm. Various reports
257 described the different shapes of Cu-NPs such as cubical (Kuo et al. 2007), rhombic
258 dodecahedral (Liang et al. 2009), 18-facet polyhedral (Lin et al. 2010), octahedral (Xu et al.
259 2011) and spherical (Noman et al. 2020), Bukhari et al 2021).

260 The XRD analysis of biosynthesized Cu-NPs showed various diffraction peaks at 44.5°,
261 51.5°, 74.75° as depicted in Figure 4A. The described peaks at 44.5°, 51.5°, 74.75° were

262 assigned to (111, 200 and 220) planes of copper. The peaks at above mentioned planes
263 confirmed the crystalline nature of Cu-NPs. There are also some extra peaks that might be due
264 to presence of some cupric oxide or copper oxide nanoparticles. The size of nanoparticles was
265 less than 27.6 nm calculated by Debye-Scherrer's formula. Tiwari *et al.* (2016) reported the
266 similar results and showed diffraction peaks of Cu-NPs at 111, 200 and 220 synthesizing from
267 *Bacillus cereus* spp. They also reported some extra peaks of copper oxide nanoparticles.
268 Similarly, Noman *et al.* (2020) and Lv *et al.* (2018) also reported the similar results showing
269 diffraction peaks at 111, 200, and 220 with a size of particles about 28.55 and 10-16 nm.

270 FTIR spectrum of biosynthesized Cu-NPs produced from *Bacillus* sp. FB-1 showed
271 peaks of absorption at 3388.72, 2928.94, 1645.23, 1403.43, 1066.48, and 595.02 cm^{-1} as shown
272 in Figure 4B. The peaks at 3388.72 and 2928.94 cm^{-1} were due to presence of OH group of
273 alcohol and C-H stretching. The peak at 1645.23 cm^{-1} was due to C=C stretching. Whereas
274 peaks at 1403.43 and 1066.48 cm^{-1} were due to bending of C-H and stretching of C-O group.
275 The presence of bands at 595.02 cm^{-1} showed probabilities of existence of copper or copper
276 oxide nanoparticles (CuO-NPs). The FTIR spectrum of biosynthesized Cu-NPs confirmed the
277 presence of alcoholic group and proteins. Coating of protein around copper nanoparticles
278 enhanced the long-term stability of particles (Valodkar *et al.*, 2011). Whereas, Noman *et al.*
279 (2020) reported the various absorption peaks at 3381.79, 2957.81, 1656.20, 1451.87, 1398.87
280 and 1111.12 cm^{-1} . The peaks at 3381.79 and 2957.81 cm^{-1} were due to presence of OH group
281 of alcohol and stretching of C-H bond. While Nieto-Maldonado *et al.*, (2022) reported the plant
282 based synthesis of copper nanoparticles and showed various absorption peaks at 3271, 2931,
283 1606, and 1029 cm^{-1} . the peaks at 3271 and 2931 cm^{-1} were due to presence of O-H and C-H
284 groups. On the other hand, the peaks at 1606 and 1029 cm^{-1} were due to C=O and C-O groups.

285 3.3 Photocatalytic Degradation of Azo Dyes

286 3.3.1 Optimization of Concentration of Cu-NPs for RB-5 Decolorization

287 In the current work, different concentrations of biosynthesized Cu-NPs were used for the
288 degradation of RB-5. After solar incubation of 4 hours, decolorization of RB-5 with 0.05, 0.1,
289 0.2, 0.5, 1, 2, 3, 4, 5, and 10 mg ml⁻¹ concentration of biosynthesized Cu-NPs was about
290 84.3±0.3%, 87.0±0.5%, 87.2±0.5%, 86.9±1.4%, 90.1±1.8%, 89.0±1.6%, 89.7±2.6%,
291 90.1±1.2%, 88.0±3.1%, and 88.5±3.4%, respectively (Figure 5). From the rate of
292 decolorization, it was clearly proved that each concentration shows maximum degradation of
293 RB-5. However, it is noteworthy that, after 1 hour incubation period, 24.9±2.9%, 45.0±0.3%,
294 60.4±1.6%, 80.5±0.8%, 80.8±1.2%, 80.8±0.2%, 81.9±0.7%, 80.9±1.3%, 81.8±2.5% and
295 75.5±2.1% decolorization of RB-5 was observed using 0.05, 0.1, 0.2, 0.5, 1, 2, 3, 4, 5, and 10
296 mg ml⁻¹ concentration of Cu-NPs. So, 0.5 mg ml⁻¹ of biosynthesized Cu-NPs was selected for
297 the decolorization of other dyes as shown in Figure 8. While Noman et al. (2020) used 1 mg
298 ml⁻¹ of Cu-NPs for the decolorization of various azo dyes. Furthermore Ahmad et al. (2018)
299 decolorized the bromophenol blue (BPB) dye using 0.25 mg ml⁻¹ of green synthesized Cu-
300 NPs.

301 Histogram correlation analysis was carried out for the selection of best concentration
302 of nanoparticles for the decolorization of dyes. In a histogram (Figure 6A) red color showed
303 non-significant while pink, grey and blue colors showed significant results. After analyzing the
304 histogram, it was observed that among all concentrations, 0.5 mg ml⁻¹ showed exceptional
305 results. When compared to 0.5 mg ml⁻¹ concentration, lower concentrations (0.05-0.2 mg ml⁻¹)
306 showed significant decolorization but not effective as 0.5 mg ml⁻¹ concentration. On the other
307 hand, higher concentrations (1 to 10 mg ml⁻¹) did not showed a proportional increase in
308 decolorization potential, especially the minimum increase was observed after the 3 hours.
309 While, 0.5 mg ml⁻¹ showed a higher initial decolorization rate and maintained throughout the
310 time, thus providing an optimum balance between effectiveness and nanoparticles
311 concentrations. So, the 0.5 mg ml⁻¹ was selected that not only conserve the resources but also

312 go with environmental and economic considerations, potentially reducing the ecological
313 footprint and material costs associated with the process of decolorization of dyes.

314 The loading plots of PCA to check ²⁹ the effect of different concentrations of nanoparticles
315 on rate of decolorization have been presented in Figure 6B. In the whole database, Dim-1 and
316 Dim-2 showed maximum contribution and occupy more than 98.5% of all databases, among
317 which Dim-1 showed 94.1 % and Dim-2 showed about 4.4 %. It was observed that
318 concentration of nanoparticles showed a significant effect on rate of decolorization.

319 3.3.2 Decolorization of Azo Dyes Using Optimized Concentration of NPs

320 After optimization, 0.5 mg ml⁻¹ concentration of biosynthesized Cu-NPs was used ³ for the
321 decolorization of various other azo dyes. The Cu-NPs were observed to carry out an effective
322 decolorization of different azo dyes (Figure 7). The results indicated that, just after solar
323 irradiation of 1/2 hour, Cu-NPs decolorized about 84.5±1.1%, 64.8±3.9%, 38.7±4.3%,
324 46.9±2.2%, 20.4±3.8% and 30.7±2.1% of RB-5, CR, MG, MB, RR-2, and BD. However,
325 71.9±1.9%, 30.5±1.4%, 61.9±3.9%, 8.1±0.5%, 15.7±2.2% and 15.9±1.6 % of RB-5, CR, MG,
326 MB, RR-2, and BD were decolorized at 50 ppm concentration of dyes just after 1/2 hour.
327 However, after 1 hour of solar incubation, decolorization of RB-5, CR, MG, MB, RR-2, and
328 BD was increased to 86.3±0.7%, 90.3±2.4%, 54.2±9.4%, 58.9±3.5%, 36.7±3.3% and
329 45.8±2.1% at 25 ppm concentration. Similarly, at 50 ppm concentration, the decolorization of
330 RB-5, CR, MG, MB, RR-2, and BD was also increased to 84.2±0.6%, 71.6±2.5%, 71.6±3.9%,
331 46.1±2.8%, 26.8±1.6% and 48.5±5.5%, after 1 of solar incubation. It is noteworthy that the
332 decolorization of the above-mentioned dyes was more at 25 ppm (Figure 7A) concentration of
333 dyes than 50 ppm (Figure 7B) concentration. Finally after 4 hours of solar irradiation, the
334 copper nanoparticles decolorized about 96.8±1.0% of RB-5, 92.2±2.2% of CR, 96.9±1.1% of
335 MG, 72.5±0.6% of MB, 58.5± 1.2% of RR-2 and 78.7±2.7% of BD at 25 ppm concentration
336 and 88.2±0.2% of RB-5, 88.5±1.9% of CR, 90.4±1.8% of MG, 64.8±1.0% of MB, 46.8±1.6%

337 of RR-2, and $67.3 \pm 2.9\%$ of BD at 50 ppm concentration. The difference in catalytic potential
338 of biosynthesized Cu-NPs for different dyes might be due to change in activity in aqueous
339 media, structure of dye, and difference in intensity of solar radiation (Noman et al., 2020). The
340 visual representation of decolorization of above-mentioned dyes has been shown in Figure S2.
341 Dyes were decolorized after the addition of biosynthesized Cu-NPs and was proved from the
342 decrease in absorption values at λ_{max} of each dye. While, (Noman et al. 2020) reported the
343 97.07%, 83.61%, 88.42%, and 90.55% decolorization of 25 ppm concentration of congo red,
344 reactive black-5, direct blue-1, and malachite green respectively. On the other hand, Ghaffar et
345 al. (2021) reported the 73.5% decolorization of Disperse yellow-125 using 0.01 %
346 concentration of dye and 0.05 % of green synthesized Cu-NPs.

347 While, the photocatalytic activity of Cu-NPs ³ for the degradation of various azo dyes such as,
348 congo red, methyl red, methylene blue (Fathima et al. 2018), and methyl orange (Li et al. 2015)
349 was also reported (Al-Hakkani, 2020). Moreover, the catalytic potential of biosynthesized
350 nanoparticles ¹ can be used for the removal of pollutants present in actual wastewater.

351 The heat map analysis was also ²⁸ carried out to check the effect of different concentration
352 of dyes over time. In a histogram (Figure 8A) red color showed non-significant while pink,
353 grey and blue colors showed significant results. After analysis it was observed that
354 for both concentrations (25 and 50 ppm), the decolorization potential of biosynthesized Cu-
355 NPs generally increased over time, with some variances among dyes. At 25 ppm concentration,
356 RB-5, CR, and MG showed high decolorization potential, reaching over 90% after 4 hours.
357 The decolorization of MB and BD also increased over time, while RR-II has the least
358 decolorization potential. On the other hand at 50 ppm concentration, RB-5 showed a consistent
359 increase in decolorization potential, but slightly lower than the 25 ppm concentration. While
360 decolorization potential of CR, MG, and BD showed significant improvements over time, and

361 MB and RR-II have moderate to low decolorization potential, thus indicating that higher
362 concentrations do not lead to better decolorization for these dyes.

363 Similarly PCA was also used to check ¹⁷ the effect of different concentrations of dyes on
364 rate of decolorization (Figure 8B). In the whole database, Dim-1 and Dim-2 showed maximum
365 contribution and occupy more than 97.3% of all databases, among which Dim-1 showed 90.2
366 % and Dim-2 showed about 7.1 %. It was observed that concentrations of dyes showed
367 significant effect on rate of decolorization over time.

368 3.3.3 Treatment of Textile Wastewater

369 The optimized concentration of Cu-NPs ⁷ was also used for the treatment of textile wastewater
370 added with CR dye (50 ppm). Before any treatment, the wastewater shows high values for
371 various parameters such as sulphates, phosphates, pH, EC, TDS, COD, and color intensity.
372 Whereas the treated wastewater showed significant reduction in all above-mentioned
373 parameters (Table 1). Few studies already reported the treatment of wastewater via metal
374 nanoparticles (Bibi et al., 2019, Dlamini et al., 2019, Al-Hakkani, 2020; Noman et al., 2020,
375 Siddique et al., 2021). ⁵ The results of present study showed that the pH of the wastewater was
376 reduced from 8.6 to 6.9 after the treatment as compared to non-treated wastewater. ⁴ The EC of
377 treated wastewater was also reduced by 59.23%. Whereas, other parameters such as TDS,
378 COD, sulfates, phosphates, and color intensity were also reduced by 57.68%, 39.66%, 43.16%,
379 49.49%, and 95.97% in comparison to non-treated wastewater as depicted in Table 1. Few
380 previous studies have also reported the treatment of wastewaters by exploiting the potential of
381 different types of nanoparticle (Bibi et al., 2019, Noman et al., 2020, Siddique et al., 2021;
382 Rasool et al., 2023; Pham-Khanh et al., 2023), For example, the findings of Siddique et al.,
383 (2021) reported the reduction in various parameters such as pH, EC, TDS, COD, and color
384 removal with the help of biologically and chemically synthesized zinc oxide nanoparticles.
385 Furthermore, Fouda et al. (2022) also reported the treatment of tanning wastewater using zinc

386 oxide nanoparticles. They reported the 96.5, 88.8, 88.5, and 91.5 % reduction in TSS, COD,
387 BOD, and conductivity of wastewater treated with zinc oxide nanoparticle. Moreover, zinc
388 oxide nanoparticles also lowered the Cr (VI) level from wastewater by 93.4 % (Fouda et al.,
389 2022). On the other hand, Noman et al. (2020) also treated the textile wastewater with the help
390 of Cu-NPs and discussed the decrease in different parameters like pH, turbidity, COD, TDS,
391 TSS, hardness, chloride, and sulphates before and after the treatment. The reduction efficiency
392 of Cu-NPs from wastewater can be attributed to functional groups, surface structure and
393 chemical components that are attached to them (Dlamini et al., 2019; Al-Hakkani, 2020). So,
394 the abovementioned results suggested that biosynthesized Cu-NPs might serve as an excellent
395 photocatalyst for the treatment of textile wastewater loaded with dyes.

396 4. Conclusion

397 Based on the findings of the current study, it might be concluded that biosynthesized Cu-NPs
398 might serve as potential agent not only for photocatalytic degradation of different textile azo
399 dyes but also for treatment of actual wastewaters by lowering sulphates, phosphates, color
400 intensity, pH, EC, TDS, and COD. Therefore, the current study emphasizes on photocatalytic
401 application of biosynthesized Cu-NPs in the decolorization of azo dyes on commercial level.

402 Acknowledgement

403 The authors extend their appreciation to the researchers supporting project number
404 8206/Punjab/NRPU/R&D/HEC/2017 funded by the Higher Education Commission of
405 Pakistan and the project No. RSP2024R469 funded by King Saud University, Riyadh, Saudi
406 Arabia.